RESEARCH ARTICLE | FEBRUARY 24 2016

# Dynamics of water confined in lyotropic liquid crystals: Molecular dynamics simulations of the dynamic structure factor FREE

Sriteja Mantha ; Arun Yethiraj



*J. Chem. Phys.* 144, 084504 (2016)
https://doi.org/10.1063/1.4942471
CHORUS

# Dynamics of water confined in lyotropic liquid crystals: Molecular dynamics simulations of the dynamic structure factor

Sriteja Mantha and Arun Yethiraj[a)]
*Theoretical Chemistry Institute and Department of Chemistry, University of Wisconsin-Madison, Madison, Wisconsin 53706, USA*

(Received 1 December 2015; accepted 8 February 2016; published online 24 February 2016)

The properties of water under confinement are of practical and fundamental interest. In this work, we study the properties of water in the self-assembled lyotropic phases of Gemini surfactants with a focus on testing the standard analysis of quasi-elastic neutron scattering (QENS) experiments. In QENS experiments, the dynamic structure factor is measured and fit to models to extract the translational diffusion constant, $D_T$, and rotational relaxation time, $\tau_R$. We test this procedure by using simulation results for the dynamic structure factor, extracting the dynamic parameters from the fit as is typically done in experiments, and comparing the values to those directly measured in the simulations. We find that the de-coupling approximation, where the intermediate scattering function is assumed to be a product of translational and rotational contributions, is quite accurate. The jump-diffusion and isotropic rotation models, however, are not accurate when the degree of confinement is high. In particular, the exponential approximations for the intermediate scattering function fail for highly confined water and the values of $D_T$ and $\tau_R$ can differ from the measured value by as much as a factor of two. Other models have more fit parameters, however, and with the range of energies and wave-vectors accessible to QENS, the typical analysis appears to be the best choice. In the most confined lamellar phase, the dynamics are sufficiently slow that QENS does not access a large enough time scale. © *2016 AIP Publishing LLC.* [http://dx.doi.org/10.1063/1.4942471]



## I. INTRODUCTION

Water plays an important role in many physical and biological processes. In many of these situations, for example, cells, nano-reactors, fuel cells, and ion-exchange resins, water is highly confined. The structural and dynamic properties of nano-confined water are very different from bulk water,[1–4] and can display either faster or slower dynamics than bulk water,[5] depending on the nature of confinement and the interaction between the water molecules and confining surfaces.

Quasi-elastic neutron scattering (QENS) has emerged as an excellent experimental tool for the study of water dynamics on molecular length-scales and time-scales.[6] QENS experiments take advantage of the fact that the neutron scattering cross section from a hydrogen atom is 20-30 times larger than that from any other nucleus. For water under confinement, for example, by surfactant or polymeric species, contrast for the hydrogen atoms of the water molecules can be increased by selectively deuterating the confining species. QENS has been extensively used to probe the dynamics of water in a wide range of applications including super-cooled water,[7–13] water confined in reverse micelles[14] or in nanopores,[15–19] in various aqueous solutions,[20–27] and in the hydration layer of biomolecules.[28–31] In this paper we study the dynamic structure factor of water confined in the self-assembled lyotropic liquid crystalline phases of Gemini surfactants using molecular dynamics simulations, with the objective of testing the approximations typically employed in the analysis of QENS experiments.

The observable in QENS measurements is the self-part of the dynamic structure factor,[32] $S_s(Q,\omega)$, which is a frequency Fourier transform of the self-part of the intermediate scattering function, $F_s(Q,t)$, defined as

$$F_s(Q,t) = \frac{1}{N}\sum_{j=1}^{N}\left\langle \exp iQ.\left[r_j(0) - r_j(t)\right]\right\rangle, \qquad (1)$$

where $Q$ is the momentum transfer variable, $N$ is the number of hydrogen atoms, and $r_j(t)$ is the position of $j$th hydrogen atom at time $t$. The dynamic structure factor (self-part) is defined as

$$S_s(Q,\omega) = \frac{1}{2\pi}\int_{-\infty}^{\infty} F_s(Q,t)e^{i\omega t}dt. \qquad (2)$$

As with any scattering measurement, inverting the dynamic structure factor to obtain the intermediate scattering function or the van Hove correlation function (inverse Q-space Fourier transform of $F_s(Q,t)$) is complicated by the finite range of $Q$ and $\omega$ accessible. Usually, a model is assumed for $F_s(Q,t)$ and the parameters in the model are fit to the experimental results for $S_s(Q,\omega)$.

The dynamics of bulk water, water in aqueous solutions, super-cooled water, and water in confinement has been studied using molecular dynamics (MD) simulations and QENS. These studies establish that the relaxation dynamics are significantly slower upon confinement or supercooling.[17,33–35] Under these conditions, translational and rotational relaxation dynamics of water show non-exponential decay.[14,33,34] It has recently been suggested that anisotropy in translational motion and molecular reorientation results in directional

a)Electronic mail: yethiraj@wisc.edu

 

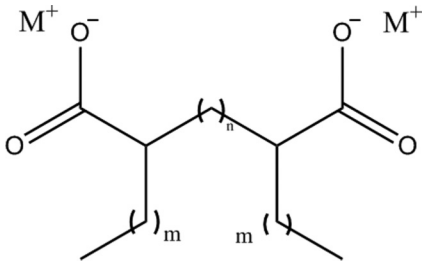


FIG. 1. Chemical formula for the dicarboxylate Gemini surfactants of this work. For Na-74, M = Na; m = 7; n = 4.

dependence of relaxational dynamics at low and high Q values, respectively.[36] Although there are many reports employing QENS based techniques, the validity of these approximations for $S_s(Q,\omega)$ and the impact on the inferred values of the translational diffusion coefficient $D_T$ and rotational relaxation time $\tau_R$ have not been tested.

We investigate the dynamics of water in lyotropic liquid crystal phases formed by the self-assembly of Gemini surfactant molecules (see Figure 1). This is an interesting system because the surface functionality and pore size can be controlled, by changing the head groups on the surfactants and the length and nature of the tails and spacers, respectively. We study the dynamics of water at room temperature (300 K) in the Na-74 system which makes hexagonal (Hex), gyroid (Gyr), and lamellar (Lam) phases at surfactant concentrations of 50 wt. % (Hex), 65 wt. % (Gyr), and 80 wt. % (Lam).[37] These three phases have different morphologies, hexagonally packed cylinders, bicontinuous network, and flat lamellae, which have positive, negative Gaussian, and flat curvature, with negatively charged carboxylate groups at the interface.

Our primary goal is to test the approximations commonly used in the analysis of QENS experiments. We find that $F_s(Q,t)$ can be factored into a translational and a rotational component, but the commonly used exponential forms for these functions are not adequate. The jump diffusion and isotropic rotation model lead to estimates for the translational diffusion constant and rotational relaxation times that are different from the actual values, and the approximations get less accurate as the degree of confinement is increased. This suggests that there are multiple relaxation processes in the dynamics of confined water. More elaborate models, however, have more parameters and therefore require more data for an adequate fit.

The rest of the paper is organized as follows: Simulation details are presented in Section II, the analysis of QENS data is described in Section III, results are presented and discussed in Section IV, and conclusions are presented in Section V.

## II. MOLECULAR DYNAMICS SIMULATIONS

We employ the molecular model used by Mondal *et al.*[38] The surfactant molecules are modeled at the united atom level using the GROMOS45a3 united atom force field,[39] the counterions and water are treated at the atomistic level using the GROMOS force field[39] and the SPC model,[40] respectively. Mixing rules for cross interactions are according to the GROMOS force field. Details of the three systems studied are in Table I.

The simulation details are as follows. Following the protocol outlined by Mondal *et al.*[38] we obtain self-assembled phases for the three concentrations, and carry out two molecular dynamics simulations for each case, at a temperature of 300 K and a pressure of 1 atm. The first simulation for all phases is a trajectory of length 2 ps where the co-ordinates are saved every 1 fs. The second simulation is a longer trajectory (6 ns for the gyroid and hexagonal phases and 30 ns for the lamellar phase) where the co-ordinates are saved less frequently (1 ps for the gyroid and hexagonal phases and 10 ps for lamellar phase). All simulations are carried out with a time step of 1 fs, using the leapfrog algorithm implemented in the GROMACS-4.5.4 software package.[41] The Lennard-Jones interactions are switched smoothly to zero at 1 nm and the particle-mesh Ewald (PME)[42,43] method is used for the Coulomb interactions. The PME parameters are as follows: real space cutoff distance of 1.4 nm and interpolation order of 6, with a maximum fast Fourier transform grid spacing of 0.12 nm. Water molecules are kept rigid using the SETTLE algorithm.[44] The pressure and temperature are maintained using a Berendsen thermostat[45] with coupling time 0.5 ps and a Berendsen barostat[45] with coupling time 1 ps.

The intermediate scattering function $F_s(Q,t)$ is calculated using Equation (1) using the short trajectory for short times, and the longer trajectory for longer times. $S_s(Q,\omega)$ is computed via a Fourier transform of the $F_s(Q,t)$ obtained from the longer trajectory.

## III. THEORY

The dynamic structure factor obtained in QENS experiments is usually analyzed by invoking a decoupling approximation for translational and rotational dynamics and using models for each of these components. In the decoupling approximation, the dynamic structure factor is a convolution of the translational and rotational contributions, i.e.,

$$\frac{S_s(Q,\omega)}{V(Q)} \cong T(Q,\omega) \otimes R(Q,\omega), \tag{3}$$

where $\otimes$ denotes a convolution in $\omega$, $V(Q)$ is the vibrational contribution modeled using a frequency independent

TABLE I. Details of systems studied. Size of confinement is defined as the width of the water channel in the self-assembled system.

| Surfactant (wt. %) | Phase | # Surfactants | # Water | Surfactants:water | Conf size (nm) |
|---|---|---|---|---|---|
| 50 | Hexagonal | 216 | 5280 | 1:24 | 1.3 |
| 65 | Gyroid | 250 | 3225 | 1:13 | 1.0 |
| 80 | Lamellar | 100 | 614 | 1:6 | 0.8 |

Debye-Waller term, and $T(Q,\omega)$ and $R(Q,\omega)$ are, respectively, the translational and rotational contributions.

The decoupling approximation can also be written in terms of the self-part of the intermediate scattering function, $F_s(Q,t)$. If $r_j = r_{CM,j} + d_j$, where $r_{CM,j}$ is the position of the center-of-mass of molecule $j$ and $d_j$ is the distance between the center-of-mass and a hydrogen atom on molecule $j$, then Equation (1) takes the form

$$F_s(Q,t) = \frac{1}{N}\sum_{j=1}^{N}\langle \exp\{iQ\left[r_{CM,j}(t) - r_{CM,j}(0)\right]\} \times \exp\{iQ\left[d_j(t) - d_j(0)\right]\}\rangle. \quad (4)$$

If the rotations and translations are de-coupled, then the average of the product is equal to the product of averages, and since the averages are independent of the molecule index, we have

$$F_s^P(Q,t) \cong F_s^T(Q,t)F_s^R(Q,t), \quad (5)$$

where

$$F_s^T(Q,t) = \langle \exp\{iQ.\left[r_{CM}(t) - r_{CM}(0)\right]\}\rangle \quad (6)$$

and

$$F_s^R(Q,t) = \langle \exp\{iQ.\left[d(t) - d(0)\right]\}\rangle. \quad (7)$$

The superscript P in Equation (5) refers to the product approximation to the intermediate scattering function.

In the jump diffusion model for the translational contribution, it is assumed that the molecule jumps a length $l$ after every time interval $\tau_0$, which gives a translational diffusion constant, $D_T = l^2/6\tau_0$. With this approximation,

$$T(Q,\omega) = \frac{1}{\pi}\frac{\gamma(Q)}{\omega^2 + \gamma^2(Q)}, \quad (8)$$

where

$$\gamma(Q) = \frac{D_T Q^2}{1 + D_T Q^2 \tau_0}. \quad (9)$$

In the isotropic rotational diffusion model, the hydrogen atom is assumed to rotate on the surface of a sphere with a radius of the O–H bond ($d = 0.98$ Å ). With this approximation

$$R(Q,\omega) = [j_0(Qd)]^2\delta(\omega) + \frac{1}{\pi}\sum_{l=1}^{\infty}(2l+1)\left[j_l(Qd)\right]^2 \times \frac{l(l+1)D_R}{\left[l(l+1)D_R\right]^2 + \omega^2}, \quad (10)$$

where $j_l$ is the spherical bessel function of order $l$, and $D_R$ is the rotational diffusion constant.

With the approximations in Equations (8)–(10),

$$\frac{S_s(Q,\omega)}{V(Q)} = [j_0(Qd)]^2\frac{1}{\pi}\frac{\gamma(Q)}{\omega^2 + \gamma^2(Q)} + \frac{1}{\pi}\sum_{l=1}^{\infty}(2l+1)\left[j_l(Qd)\right]^2 \times \frac{\gamma(Q) + l(l+1)D_R}{\left[\gamma(Q) + l(l+1)D_R\right]^2 + \omega^2}. \quad (11)$$

In principle, Equation (11) is an approximate expression for $S_s(Q,\omega)$ that can be fit to experimental QENS measurements. In practice, short times of the order 0.1 ps are not accessible to QENS experiments and these are usually incorporated as prefactors into the analytical expression, i.e.,

$$S_s(Q,\omega) = A_0 T_{Sh}(Q)\left\{[j_0(Qd)]^2\frac{\gamma(Q)}{\omega^2 + \gamma^2(Q)}\right\} + A_0 T_{Sh}(Q)\left\{\sum_{l=1}^{\infty}(2l+1)\,R_{Sh,l}\left[j_l(Qd)\right]^2\frac{\gamma(Q) + l(l+1)D_R}{\left[\gamma(Q) + l(l+1)D_R\right]^2 + \omega^2}\right\}, \quad (12)$$

where $T_{Sh}(Q)$ and $R_{Sh,l}$ are prefactors corresponding to short time translational and rotational relaxation dynamics, assumed to originate from local harmonic motions of a water molecule trapped in a cage. Following Faraone *et al.*,[46] we model $T_{Sh}(Q)$ as an effective Debye-Waller factor, with mean square amplitude a = 0.4 Å, i.e,

$$T_{Sh}(Q) = \exp\left\{\frac{-Q^2a^2}{3}\right\}. \quad (13)$$

$R_{Sh,l}$ is obtained by first computing $l$th order rotational auto-correlation function, which is fit to an expression suggested by Chen *et al.*[35] This function reaches a constant value within 0.1 ps, and we set $R_{Sh,l}$ equal to the constant value. (Note that $V(Q)$ is not present because we use a rigid model for water.) In the experimental analysis, the instrument resolution function is convoluted with Equation (12) to fit to scattering data. Since our "data" are obtained from MD simulations, an instrument resolution function is not necessary.

There are three approximations inherent to Equation (12): (i) decoupling of translational and rotational contributions, (ii) jump diffusion model for translation, and (iii) isotropic model for rotations. There are three adjustable parameters, namely, $D_R$, $D_T$, and $\tau_0$, which can be fit to experiment. We define a rotational relaxation time, $\tau_R$, by $\tau_R \equiv 1/6D_R$.

## IV. RESULTS AND DISCUSSION

### A. Dynamic structure factor

The self-part of dynamic structure factor[32] gives information about single molecule relaxation dynamics. The width of this function is affected by both the rotational and

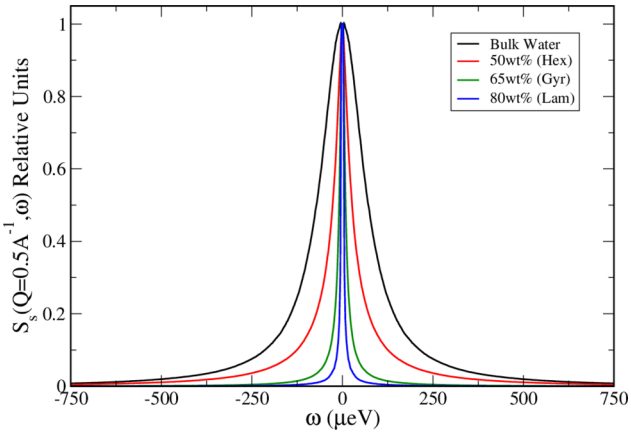


FIG. 2. Simulation results for $S_s(Q,\omega)$ for pure water and for water in the different self-assembled phases for Q = 0.5 Å$^{-1}$.

translational diffusion of the molecule, and faster dynamics (larger diffusion constants or higher $Q$) give a larger width in the dynamic structure factor.

The width of the dynamic structure factor is greatest for bulk water and decreases as the surfactant concentration is increased. Figure 2 depicts $S_s(Q,\omega)$ in each phase, normalized to the value at the peak, for Q = 0.5 Å$^{-1}$. The relaxation dynamics become slower as the surfactant concentration is increased, reflecting slower dynamics of water under confinement. This could be attributed to the greater structure in water, manifested by a stronger peak in the pair correlation function,[38] or the increasing degree of confinement going from the hexagonal to the gyroid to the lamellar phase.

### B. Decoupling of translational and rotational relaxations

The simulations show that the decoupling approximation is accurate for all the phases for a range of wave-vectors and times. We compute $F_s(Q,t)$, $F_s^R(Q,t)$, and $F_s^T(Q,t)$ in the simulations. Figure 3 compares the simulation results for $F_s(Q,t)$ to $F_s^P(Q,t)$ for three different values of Q in the gyroid phase. Similar results are seen for bulk water and for water in the other phases, which are therefore not shown. The decoupling approximation works quite well in all cases, with slight discrepancies at longer times and larger values of Q.

### C. Analysis of $S_s(Q,\omega)$ in the manner of QENS experiments

We analyze the simulation results for $S_s(Q,\omega)$ in the same fashion as done in QENS experiments, thus treating the simulation results as "data." We fit simulation results for $S_s(Q,\omega)$ using the analytical expression (Equation (12)) to extract $D_T$, $\tau_R$, and $\tau_0$, using the trust region algorithm,[47] a non-linear least squares fitting algorithm in MATLAB.[48] We use $S_s(Q,\omega)$ at six different Q values in the range 0.3–1.3 Å$^{-1}$ for bulk water and 0.5–2.5 Å$^{-1}$ for confined water. The fit functions are compared to the simulation results for $S_s(Q,\omega)$ in Figure 4 for $Q$ = 0.9 Å$^{-1}$ and $Q$ = 1.7 Å$^{-1}$, in the gyroid phase. These two Q values summarize the trends observed for the confined water systems at low and high Q values, respectively. From the figure, it is observed that at low Q, where the relaxation dynamics is predominantly governed by translational motion, Equation (12) describes $S_s(Q,\omega)$ very well. On the other hand, at high Q values where both translational and rotational motions make a significant contribution to the relaxation dynamics, Equation (12) gives a slightly narrower peak than that obtained directly from MD simulations. In contrast to what we see for confined water, for bulk water Equation (12) describes $S_s(Q,\omega)$ remarkably well for all values of Q.

The translation diffusion coefficient ($D_T$) obtained from the fit to $S_s(Q,\omega)$ using the jump-diffusion isotropic rotation (JDIR) model is in excellent agreement with simulation results for pure water, but the agreement becomes progressively poorer as the degree of confinement increases. On the other hand, values obtained for rotational relaxation time ($\tau_R$) differ significantly when compared to corresponding simulation results. The simulation results for $D_T$ are obtained from the linear regime in the mean square displacement. To compute $\tau_R$, we compute the second order water dipole moment autocorrelation function and define $\tau_R$ as the integral of this function. The values obtained from the fit are compared to simulation results in Table II. For $D_T$, the agreement between simulation results and the fit is excellent for bulk water, but is not as good for confined water and for the lamellar phase is off by almost a factor of two. Similarly, for $\tau_R$ the agreement between simulation results and the fit becomes poorer as the degree of confinement is increased. Interestingly, $\tau_R$ for bulk water obtained from fit parameters is a factor of two higher than that observed in simulations. We attribute this to faster



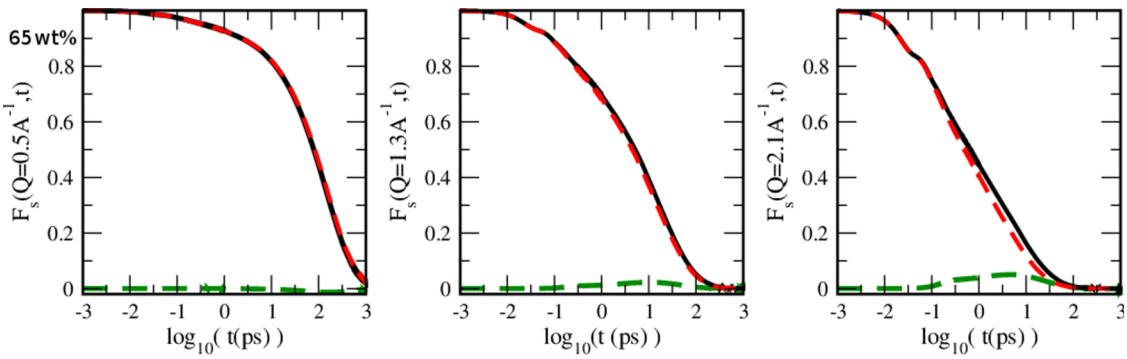


FIG. 3. Comparison of simulation results for the intermediate structure factor $F_s(Q,t)$ (black lines), to that obtained using the decoupling approximation $F_s^P(Q,t) = F_s^T(Q,t)F_s^R(Q,t)$ (red dashed lines), for three different values of Q. The green lines are $F_s^P(Q,t)$–$F_s(Q,t)$.

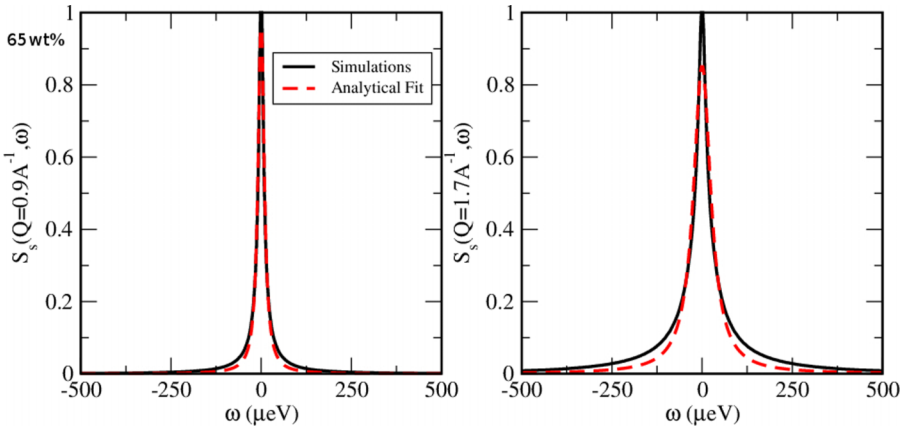


FIG. 4. Comparison of simulation results (black lines) for $S_s(Q,\omega)$ to the fit using Equation (12) (red dashed lines) in the gyroid phase.

translational dynamics in bulk water, which dominates the width of $S_s(Q,\omega)$, thereby masking the contribution from rotational relaxation dynamics. The results for $\tau_R$ do not change significantly (within statistical uncertainties) when a flexible water model[49] is used.

### D. Breakdown of jump diffusion (JD) and isotropic rotation (IR) models

The JD and IR models break down for water under confinement. In the jump diffusion and isotropic rotation models,

$$F_s^{T,JD}(Q) = \exp\{-\gamma(Q)t\}, \tag{14}$$

$$F_s^{R,IR}(Q) = [j_0(Qd)]^2 + \sum_{l=1}^{\infty}(2l+1)[j_l(Qd)]^2 \times \exp\{-l(l+1)D_R t\}. \tag{15}$$

These expressions can be compared directly to simulations to test their validity. We also consider stretched exponential approximations

$$F_s^{T,st}(Q) = \exp\left\{-(\gamma_{str}(Q)t)^{\beta_T}\right\}, \tag{16}$$

$$F_s^{R,st}(Q) = [j_0(Qd)]^2 + \sum_{l=1}^{\infty}(2l+1)[j_l(Qd)]^2 \times \exp\left\{-(l(l+1)D_{R,str}t)^{\beta_R}\right\}, \tag{17}$$

which contain two additional parameters $\beta_T$ and $\beta_R$. From the definition of isotropic rotational relaxation model, $[j_0(Qd)]^2$ in Equations (15) and (17) corresponds to the value to which $F_s^R(Q,t)$ stabilizes as $t \to \infty$. There were reports[12,50] in the literature suggesting $\left(\frac{3[j_1(Qd)]}{Qd}\right)^2$ as better representation for $F_s^R(Q,t\to\infty)$. However, for the systems studied in this work $[j_0(Qd)]^2$ describes $F_s^R(Q,t\to\infty)$ very well compared to $\left(\frac{3[j_1(Qd)]}{Qd}\right)^2$, and we therefore use the former in the analysis.

The jump diffusion and isotropic rotation models do not capture the relaxation of the intermediate scattering function, and stretched exponential forms provide a better fit. Figure 5, which compares the exponential and stretched exponential forms for the translational and rotational parts to simulations in the gyroid, shows that the exponential forms show deviations from the simulations, but the stretched exponential forms provide a good fit for all times.

The good fit provided by stretched exponential forms suggests that there are multiple relaxation processes for confined water.[28,51–53] These could be caused by different populations, for example, water near the head groups and in the middle of the pores, or by anisotropy of the matrix, for example, the dynamics along the pores is different from that in the direction perpendicular to the pores. These effects become more significant as the degree of confinement is increased. If multiple relaxation processes have significantly different relaxation times, the stretching exponents ($\beta_R$ and $\beta_T$) deviate from unity. An estimate of the degree of non-exponentiality can be obtained by examining the stretching exponents obtained from the fit. Table III lists the $\beta_R$ and $\beta_T$ values we obtain from the fit. The $\beta_R$ values are only weakly sensitive to Q, but $\beta_T$ values decrease as Q is increased, suggesting translational relaxation becomes more non-exponential at short length scales.

The $D_T$ obtained from a fit to the stretched exponential function is, however, not in better agreement with simulations than the JDIR model. We obtain $D_T$ from the stretched exponential fit using the relations[21,23,25]

$$\bar{\tau} = \frac{1}{\gamma^{str}\beta_T}\Gamma\left(\frac{1}{\beta_T}\right), \tag{18}$$

$$\bar{D_T} = \frac{1}{\bar{\tau}Q^2}, \tag{19}$$

and the results from the fit are compared to simulation results and results from the exponential fit in Table IV. The fit values do not represent an improvement over the exponential model.

TABLE II. Comparison of simulation results for $D_T$ and $\tau_R$ to fits to the dynamic structure factor using Equation (12).

| | $D_T$ ($\times 10^{-5}$ cm$^2$ s$^{-1}$) | | $\tau_R$ (ps) | |
|---|---|---|---|---|
| System | Simulation result | Fit to $S_s(Q,\omega)$ | Simulation result | Fit to $S_s(Q,\omega)$ |
| Bulk water | 4.3 ± 0.1 | 4.2 ± 0.2 | 0.87 ± 0.03 | 1.7 ± 0.3 |
| Hexagonal | 0.83 ± 0.04 | 0.8 ± 0.1 | 6.31 ± 0.06 | 4.2 ± 0.7 |
| Gyroid | 0.21 ± 0.01 | 0.17 ± 0.02 | 20.10 ± 0.80 | 15 ± 2 |
| Lamellar | 0.04 ± 0.01 | 0.08 ± 0.06 | 155.83 ± 7.00 | 104 ± 80 |

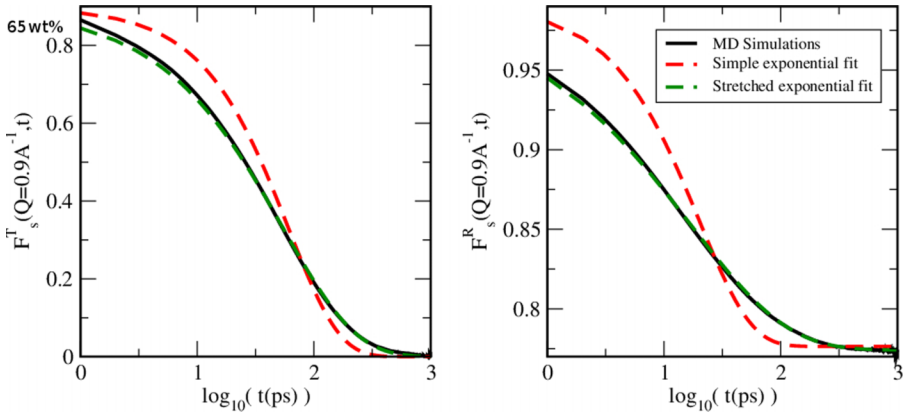


FIG. 5. Fit of simulation results (black lines) for (a) $F_S^T(Q,t)$ and (b) $F_S^R(Q,t)$ to exponential form of Equations (14) and (15) (red lines) and stretched exponential forms of Equations (16) and (17) (green lines) for the gyroid phase.

Note that Equation (19) is valid only if $\bar{\tau} \propto Q^{-2}$. This is nearly the case for water in the Hex ($\bar{\tau} \propto Q^{-1.95}$) and Gyroid ($\bar{\tau} \propto Q^{-1.88}$) phases, but not in the Lam phase ($\bar{\tau} \propto Q^{-1.45}$).

Water under confinement is often analyzed by assuming two populations of the water molecules, namely, bound and free, which can be defined using the distance from the surface. Such an analysis has been used successfully to study water in silica pores.[36,54–57] In the LLC systems, however, we are not able to distinguish between "free" and "bound" water molecules. For a low degree of confinement, i.e., hexagonal morphology, the dynamics of water is sufficiently fast that the residence time at the surface is not large. For a higher degree of confinement, i.e., in the gyroid and lamellar morphologies, the diameter of water channel is less than a nanometer, which makes most of the water molecules "bound" to the surface.

### E. Relaxation time scales in different confined water systems and accessibility of QENS experiments

From the accessible time-scales, we conclude that QENS experiments can be safely used to study water in the hexagonal and gyroid morphologies, but the lamellar morphology poses a challenge. Figure 6 depicts $F_s(Q,t)$ for the three morphologies at the lowest Q studied, and shows that the function decays to zero at 0.75 ns, 1.5 ns, and 12 ns, in the Hex, Gyr, and Lam morphologies, respectively. (At the highest Q studied, the corresponding times are 50 ps, 250 ps, and 2.5 ns.) For comparison, the time window accessible to QENS experiments is 4 ps-2 ns.[46,58,59] It would therefore be useful to explore techniques that go to longer time scales.[46,60]

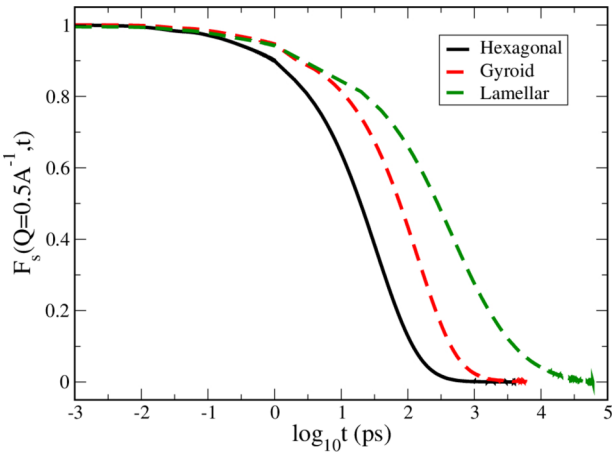


FIG. 6. Self-intermediate structure, $F_s(Q,t)$, computed from water confined in hexagonal, gyroid, and lamellar morphologies at the lowest Q explored in this work.

TABLE III. Values of $\beta_R$ and $\beta_T$ obtained from fits to Equations (16) and (17). For bulk water S(Q,$\omega$) is computed for six different Q values between 0.3 and 1.3 Å$^{-1}$. The values of $\beta_T$ and $\beta_R$ computed at other three Q values (not reported above) are ~0.90.

| | $\beta_T$ | | | | $\beta_R$ | | | |
|---|---|---|---|---|---|---|---|---|
| Q (Å$^{-1}$) | Bulk | Hex | Gyr | Lam | Bulk | Hex | Gyr | Lam |
| 0.5 | 0.88 | 0.64 | 0.71 | 0.46 | 0.90 | 0.61 | 0.52 | 0.32 |
| 0.9 | 0.90 | 0.63 | 0.65 | 0.38 | 0.91 | 0.55 | 0.53 | 0.33 |
| 1.3 | 0.91 | 0.60 | 0.59 | 0.34 | 0.93 | 0.55 | 0.53 | 0.33 |
| 1.7 | ... | 0.57 | 0.53 | 0.32 | ... | 0.56 | 0.54 | 0.33 |
| 2.1 | ... | 0.55 | 0.49 | 0.30 | ... | 0.57 | 0.56 | 0.34 |
| 2.5 | ... | 0.53 | 0.46 | 0.29 | ... | 0.58 | 0.58 | 0.34 |

TABLE IV. Values of $D_T$ obtained from fits to Equations (19) and (12).

| | $D_T$ ($\times 10^{-5}$ cm$^2$ s$^{-1}$) | | |
|---|---|---|---|
| System | Simulation result | Fit to stretched exponential (Eq. (19)) | Fit to exponential (Eq. (12)) |
| Hex | 0.83 ± 0.04 | 0.81 ± 0.04 | 0.8 ± 0.1 |
| Gyr | 0.21 ± 0.01 | 0.18 ± 0.01 | 0.17 ± 0.02 |
| Lam | 0.040 ± 0.005 | 0.013 ± 0.003 | 0.08 ± 0.06 |

## V. SUMMARY AND CONCLUSION

We test the approximations commonly used in the analysis of QENS experiments of confined water. We perform molecular dynamics simulations of water confined in the lyotropic phases of Gemini surfactants and monitor the dynamic structure factor and other dynamic properties. By analyzing the simulations in the same manner as experiments, and comparing to the exact (in the simulation) values, we are able to test the approximations in the analysis.

We find that the de-coupling approximation, where the self-part of the intermediate scattering function is factored into a product of translational and rotational components is quite accurate in all the three phases (hexagonal, gyroid, and lamellar), and for all the wave-vectors tested. The jump

diffusion model and the isotropic rotation model, however, do not capture the dynamics and get progressively less accurate as the degree of confinement increases. In particular, the exponential approximation to the translational and rotational intermediate scattering functions is faulty. These functions are better represented as stretched exponentials emphasizing that multiple relaxation process become important as the degree of confinement increases.

Our analysis suggests that standard analysis of QENS measurements provides a qualitative understanding of the water dynamics, i.e., the trends are all correct, but for a more quantitative understanding, one should consider models with multiple relaxation processes. A stretched exponential model fits the intermediate scattering functions but the extracted diffusion coefficient is not accurate. On the other hand, there are insufficient data in one experiment to fit models, e.g., a sum of exponentials, that have additional parameters. Under the circumstances, the standard analysis of QENS experiments is probably the best available choice.

We also show that water under extreme confinement (pore size $\leq 0.8$ nm) has sufficiently slow dynamics that experiments with a longer time window would be valuable. In the lamellar phase, for example, the intermediate scattering function decays to zero over a time-scale of 12 ns, which is beyond the 4 ps-2 ns time accessible to QENS with currently accessible energy scales. A fit to the short-time behavior is therefore risky given the multiple dynamic processes that are at play.

## ACKNOWLEDGMENTS

This material is based upon work supported by the Department of Energy under Award No. DE-SC0010328. We acknowledge computational support through Extreme Science and Engineering Discovery Environment (XSEDE) allocations under Grant No. TG-CHE090065. We acknowledge support from the UW Madison chemistry department cluster under Grant No. CHE-0840494 and compute resources and assistance of the UW-Madison Center for High Throughput Computing (CHTC). We are also grateful to Dr. Antonio Faraone, Dr. Kenneth Herwig, Dr. Eugene Mamontov, and Professor Mahesh Mahanthappa for helpful discussions. We thank Dr. Jagannath Mondal for sharing with us different input files for setting up initial simulations.

[1]H. Ye, H. Zhang, Y. Zheng, and Z. Zhang, Microfluid. Nanofluid. **10**, 1359 (2011).
[2]H. Stanley, S. Buldyrev, G. Franzese, P. Kumar, F. Mallamace, M. Mazza, K. Stokely, and L. Xu, J. Phys.: Condens. Matter **22**, 284101 (2010).
[3]M. C. Gordillo, G. Nagy, and J. Mart, J. Chem. Phys. **123**, 054707 (2005).
[4]S. Park, D. E. Moilanen, and M. D. Fayer, J. Phys. Chem. B **112**, 5279 (2008).
[5]J. C. Rasaiah, S. Garde, and G. Hummer, Annu. Rev. Phys. Chem. **59**, 713 (2008).
[6]M. Bee, *Quasielastic Neutron Scattering:Principles and Applications in Solid State Chemistry, Biology and Materials Science* (CRC Press, 1988).
[7]S.-H. Chen, J. Teixeira, and R. Nicklow, Phys. Rev. A **26**, 3477 (1982).
[8]J. Teixeira, M.-C. Bellissent-Funel, S. H. Chen, and A. J. Dianoux, Phys. Rev. A **31**, 1913 (1985).
[9]D. Di Cola, A. Deriu, M. Sampoli, and A. Torcini, J. Chem. Phys. **104**, 4223 (1996).
[10]J. Teixeira, A. Luzar, and S. Longeville, J. Phys.: Condens. Matter **18**, S2353 (2006).
[11]A. Cunsolo, A. Orecchini, C. Petrillo, and F. Sacchetti, J. Chem. Phys. **124**, 084503 (2006).
[12]J. Qvist, H. Schober, and B. Halle, J. Chem. Phys. **134**, 144508 (2011).
[13]J. Teixeira, M.-C. Bellissent-Funel, and S. H. Chen, J. Mol. Liq. **48**, 111–121 (1991).
[14]M. R. Harpham, B. M. Ladanyi, N. E. Levinger, and K. W. Herwig, J. Chem. Phys. **121**, 7855 (2004).
[15]M.-C. Bellissent-Funel, S. H. Chen, and J.-M. Zanotti, Phys. Rev. E **51**, 4558 (1995).
[16]V. Crupi, D. Majolino, P. Migliardo, and V. Venuti, J. Phys. Chem. B **106**, 10884 (2002).
[17]A. Faraone, L. Liu, C.-Y. Mou, P.-C. Shih, J. R. D. Copley, and S.-H. Chen, J. Chem. Phys. **119**, 3963 (2003).
[18]L. Liu, A. Faraone, C. Mou, C. Yen, and S. Chen, J. Phys.: Condens. Matter **16**, S5403 (2004).
[19]P. Gallo, Phys. Chem. Chem. Phys. **2**, 1607 (2000).
[20]F. Cavatorta, F. Deriu, D. D. Cola, and H. D. Middendorf, J. Phys.: Condens. Matter **6**, A113 (1994).
[21]M. Feeney, C. Brown, A. Tsai, D. Neumann, and P. G. Debenedetti, J. Phys. Chem. B **105**, 7799 (2001).
[22]V. Calandrini, A. Deriu, G. Onori, R. Lechner, and J. Pieper, J. Chem. Phys. **120**, 4759 (2004).
[23]H. N. Bordallo, K. W. Herwig, B. M. Luther, and N. E. Levinger, J. Chem. Phys. **121**, 12457 (2004).
[24]M. R. Harpham, N. E. Levinger, and B. M. Ladanyi, J. Phys. Chem. B **112**, 283 (2008).
[25]M. Nakada, K. Maruyama, O. Yamamuro, and M. Misawa, J. Chem. Phys. **130**, 074503 (2009).
[26]E. Mamontov, J. Phys. Chem. B **113**, 14073 (2009).
[27]P. B. Ishai, E. Mamontov, J. D. Nickels, and A. P. Sokolov, J. Phys. Chem. B **117**, 7724 (2013).
[28]M.-C. Bellissent-Funel, J.-M. Zanotti, and S. H. Chen, Faraday Discuss. **103**, 281 (1996).
[29]D. I. Svergun, S. Richard, M. Koch, Z. Sayers, S. Kuprin, and G. Zaccai, Proc. Natl. Acad. Sci. U. S. A. **95**, 2267 (1998).
[30]D. Russo, G. Hura, and T. Head-Gordon, Biophys. J. **86**, 1852 (2004).
[31]J. Nickels, H. O'Neill, L. Hong, M. Tyagi, G. Ehlers, K. L. Weiss, Q. Zhang, Z. Yi, E. Mamontov, J. Smith, and A. Sokolov, Biophys. J. **103**, 1566 (2012).
[32]P. Egelstaff, *An Introduction to the Liquid State* (Oxford University Press, 1992).
[33]S.-H. Chen, P. Gallo, F. Sciortino, and P. Tartaglia, Phys. Rev. E **56**, 4231 (1997).
[34]S. H. Chen, C. Liao, F. Sciortino, P. Gallo, and P. Tartaglia, Phys. Rev. E **59**, 6708 (1999).
[35]L. Liu, A. Faraone, and S.-H. Chen, Phys. Rev. E **65**, 041506 (2002).
[36]A. A. Milischuk, V. Krewald, and B. M. Ladanyi, J. Chem. Phys. **136**, 224704 (2012).
[37]G. P. Sorenson, K. L. Coppage, and M. K. Mahanthappa, J. Am. Chem. Soc. **133**, 14928 (2011).
[38]J. Mondal, M. Mahanthappa, and A. Yethiraj, J. Phys. Chem. B **117**, 4254 (2013).
[39]L. D. Schuler, X. Daura, and W. F. van Gunsteren, J. Comput. Chem. **22**, 1205 (2001).
[40]H. Berendsen, J. Postma, W. van Gunsteren, and J. Hermans, in *Intermolecular Forces*, edited by B. Pullman, The Jerusalem Symposia on Quantum Chemistry and Biochemistry (Springer, Netherlands, 1981), Vol. 14, pp. 331–342.
[41]B. Hess, C. Kutzner, D. Van der Spoel, and E. Lindahl, J. Chem. Theory Comput. **4**, 435 (2008).
[42]T. Darden, D. York, and L. Pedersen, J. Chem. Phys. **98**, 10089 (1993).
[43]U. Essmann, L. Perera, M. L. Berkowitz, T. Darden, H. Lee, and L. G. Pedersen, J. Chem. Phys. **103**, 8577 (1995).
[44]S. Miyamoto and P. A. Kollman, J. Comput. Chem. **13**, 952 (1992).
[45]H. J. C. Berendsen, J. P. M. Postma, W. F. van Gunsteren, A. DiNola, and J. R. Haak, J. Chem. Phys. **81**, 3684 (1984).
[46]A. Faraone, E. Fratini, A. M. Todea, B. Krebs, A. Müller, and P. Baglioni, J. Phys. Chem. C **113**, 8635 (2009).
[47]J. J. Moré and D. C. Sorensen, SIAM J. Sci. Stat. Comput. **4**, 553 (1983).
[48]Matlab, version 7.10.0 (R2010a), The MathWorks Inc., Natick, Massachusetts, 2010).
[49]Y. Wu, H. Tepper, and G. Voth, J. Chem. Phys. **124**, 024503 (2006).
[50]F. Volino, J.-C. Perrin, and S. Lyonnard, J. Phys. Chem. B **110**, 11217 (2006).

[51]S. Mitra, R. Mukhopadhyay, I. Tsukushi, and S. Ikeda, J. Phys.: Condens. Matter **13**, 8455 (2001).
[52]L. M. Anovitz, E. Mamontov, P. ben Ishai, and A. I. Kolesnikov, Phys. Rev. E **88**, 052306 (2013).
[53]M.-C. Bellissent-Funel, J. Teixeira, K. Bradley, S.-H. Chen, and H. Crespi, Phys. B **180**, 740 (1992).
[54]P. Gallo, M. Rovere, and S.-H. Chen, J. Phys. Chem. Lett. **1**, 729 (2010).
[55]I. Bourg and C. Steefel, J. Phys. Chem. C **116**, 11556 (2012).
[56]P. Gallo, M. Rovere, and S.-H. Chen, J. Phys.: Condens. Matter **24**, 064109 (2012).
[57]M. Rovere and P. Gallo, J. Phys.: Condens. Matter **15**, S145 (2003).
[58]J. R. D. Copley and J. C. Cook, Chem. Phys. **292**, 477 (2003).
[59]A. Meyer, R. M. Dimeo, P. M. Gehring, and D. A. Neumann, Rev. Sci. Instrum. **74**, 2759 (2003).
[60]N. Rosov, M. Rathgeber, and S. Monkenbusch, ACS Symp. Ser. **739**, 103 (2000).